
Article:
Ahmad, S., Pilakoutas, K., Khan, Q.U.Z. et al. (1 more author) (2014) Stress-Strain Model for Low-Strength Concrete in Uni-Axial Compression. Arabian Journal for Science and Engineering, 40 (2). 313 - 328. ISSN 1319-8025

https://doi.org/10.1007/s13369-014-1411-1

Ahmad, S., Pilakoutas, K., Khan, Q.U.Z. & Neocleous, K. (2014) "Stress–Strain Model for Low-Strength Concrete in Uni-Axial Compression", Arabian Journal for Science and Engineering, 40(2), 313-328. DOI: 10.1007/s13369-014-1411-1

Stress-Strain Model for Low Strength Concrete in Uni-axial Compression

Sohaib Ahmad[1], Kypros Pilakoutas[1*], Qaiser uz Zaman Khan[2], and Kyriacos Neocleous[1]

[1] Dept. of Civil and Structural Engineering, University of Sheffield, Sheffield, UK

[2] Dept. of Civil and Structural Engineering, University of Engineering and Technology, Taxila, Pakistan

[*]Corresponding author: Department of Civil and Structural Engineering, The University of Sheffield, Sir Frederick Mappin Building, Mappin Street, S1 3JD, Sheffield, UK. T. +44 114 222 5065, F. +44 114 222 5700. E-mail: k.pilakoutas@sheffield.ac.uk

ABSTRACT

One of the most significant problems found in non-engineered reinforced concrete structures is poor quality concrete. Due to this problem, these structures are fragile and can lead to brittle failure modes even for small magnitude earthquakes. The statistics of different post-earthquake surveys indicate that the reinforced concrete building stock in developing countries can have a broad range of low strength concrete, which can vary between 4 to 20MPa. The lack of information regarding low strength concrete (4 to 20MPa) mechanical characteristics necessitates a study on low strength concrete and the development of appropriate stress-strain models to realistically simulate the inelastic behaviour of non-engineered structures. This paper presents the methods adopted to produce low strength concrete in the laboratory. The stress-strain results obtained from compression tests on cylindrical concrete specimens are presented and new expressions for the modulus of elasticity, peak strain and failure strain are developed. These expressions are used in the development of a stress-strain model for low strength concrete which can be used for analytical vulnerability assessment of non-engineered reinforced concrete structures.

***Keywords**: Non-engineered reinforced concrete structures, Low Strength Concrete, Mechanical properties, Compressive strength, Elastic Modulus*

Nomenclature

E_c modulus of elasticity of concrete

E_{chord} chord modulus of elasticity

E_{sec} secant modulus

E_p secant modulus of concrete corresponding to $f_c^{'}$

α mean stress factor

f_{c85} stress at 85% of the $f_{c\max}$

$f_{c,ult}$ ultimate concrete strength

$f_{c\max}$, $f_c^{'}$ concrete compressive strength

f_c concrete stress

f_{cmean} mean compressive strength

f_{resd} residual concrete strength

ε_{cmax} strain corresponding to concrete compressive strength

ε_{cult} ultimate (failure) concrete strain

ε_{c85} strain corresponding to f_{c85}

μ mean

σ standard deviation

1 Introduction

Reinforced Concrete (RC) structures in developing countries suffer from poor quality control and poor construction practices. Different post earthquake reconnaissance reports from developing countries, e.g. Pakistan [1-4], revealed the imprudent use of poor materials, bad design and inappropriate construction practices. Hence, structures constructed with such materials and such practices can be considered to be essentially non-engineered [2]. Most of the collapsed RC structures as a result of the Kashmir earthquake had a mean concrete compressive strength ($f_c^{'}$) of around 15MPa [2]. Moreover, results of Schmidt hammer tests on RC buildings with different damage levels in the Khyber Pakhtunkhwa province of Pakistan showed that the $f_c^{'}$ for the collapsed RC buildings varied between 7 and 22 MPa [3]. Similar evidence was also reported in Turkey where testing of concrete cores, taken from 35 RC buildings after the 1995 Dinar earthquake, indicated that the mean $f_c^{'}$ was around 10 MPa [5]. More recently, an assessment of the $f_c^{'}$ of 1178 RC buildings, located around Istanbul, showed that the mean $f_c^{'}$ was around 17 MPa, whilst 16% of the buildings had strength below 8 MPa [6].

The in-elastic behaviour of Non-Engineered Reinforced Concrete (NERC) buildings has not been studied much in the past and most researchers (e.g. Kyriakides [7]) assume that the behaviour of Low Strength Concrete (LSC) is similar to that of Normal Strength Concrete (NSC). Given the fact that LSC is not an engineered material, but rather the result of necessity, it is natural to expect it to have a higher variability than normal concrete. Furthermore, due to the brittle failures encountered in NERC buildings, it is also natural to suspect brittle material characteristics from such concrete. Many stress-strain (σ-ε) relationships can be found in the published literature for unconfined normal and high strength concrete subjected to uni-axial compressive loading [8-16], however, the performance of existing stress-strain models using LSC experimental data in the range of 5 to 15 MPa has not been confirmed.

Concrete σ-ε relationships are in general developed empirically and aim to satisfy certain boundary conditions, such as the initial stiffness 'E_c' and zero stiffness at peak load. Most researchers define the entire σ-ε curve by using a single expression and adopt suitable parameters that control the shape of the ascending and descending branch [12-14, 16]. Others adopt two separate relationships for each branch [15, 17]. In most existing studies the behaviour of the ascending branch is very well defined as compared to the descending (degrading) branch and conflicting degrading behaviour can be obtained from different models. This necessitates the careful reappraisal of the degrading behaviour of LSC and in particular of the σ-ε descending branch.

This paper aims to study the above issues and initially starts by describing the experimental setup and procedure for the tests carried out on a variety of LSC mixes. This is followed by the analysis of the results which are used to develop expressions for maximum compressive strength (f_{cmax}), elastic modulus (E_c), the peak strain (ε_{cmax}) and ultimate strain (ε_{cult}). Since, various σ-ε formulations in the literature fulfil satisfactorily the mathematical requirements of the basic boundary conditions, the foucs of the current study is to investigate their suitability for LSC. The best model is selected and by using the newly developed expressions a simple σ-ε model is developed for LSC.

2 Materials and Methods

2.1 Preparation of LSC mixes

LSC with various compressive strength ranges was successfully formulated in the laboratories of the University of Sheffield (UoS), U.K. and the University of Engineering and Technology (UET), Taxila, Pakistan [18]. Different mixes were adopted to achieve a broad range of LSC by considering the deficiencies observed in non-engineered construction sites in Pakistan. These deficiencies are generally a result of the use of high water to cement ratio (w/c in the range of 0.75 to 0.8), no or limited curing, low quality aggregates, low cement content and high sand ratios as well as poor compaction. Five different LSC ranges were prepared using different mixes. The main variables

were: mix proportion [cement (C), sand (S) and aggregate (A)], w/c ratio, curing, recycled aggregates and air entraining (AE) agent.

2.1.1 Concrete mix details

The ACI mix design method has provisions for producing concrete with strength down to 13.8 MPa by using a W/C ratio of 0.82 [19], thus these provisions were adopted for the initial concrete mix design. The details of the thirteen different LSC mixes (M_1-M_{13}) made at the UoS are provided in Table 1. At UET, specimens were prepared from M_4 mix only.

Table 1 Details of the various mixes used for making LSC

MIX	C	S	A	W/C	C:S:A	Curing	AE
	kg/m^3	kg/m^3	kg/m^3			days	% of cement
M_1	293	634	1188	0.82	1:2.2:4	-	-
M_2	267	792	1056	0.90	1:3:4	-	-
M_3	313	619	1188	0.75	1:2:3.8	5	-
M_4	293	766	1056	0.82	1:2.6:3.6	5	-
M_5	269	864	1023	0.74	1:3.2:3.8	-	-
M_6	269	864	1023	0.74	1:3.2:3.8	5	-
M_7	340	860	1035	0.5	1:2.5:3.0	-	3.5
M_8	310	860	1035	0.55	1:2.8:3.3	-	2.5
M_9	313	619	1188	0.75	1:2:3.8	5	
M_{10}	313	619	1188	0.75	1:2:3.8	14	
M_{11}	340	860	*1035	0.5	1:2.5:3.0	-	3.5
M_{12}	310	860	*1035	0.55	1:2.8:3.3	-	2.5
M_{13}	340	860	1035	0.5	1:2.5:3.0	5	3.5

*Recycled aggregate

Mixes M_1 and M_2 have a very high w/c ratio and the specimens were not cured. M_3 and M_4 have a relatively lower w/c ratio and the specimens were cured for 5 days. M_5 and M_6 have a high sand proportion and slightly reduced cement content as compared to M_3 and M_4, to allow the mix to be more workable. Specimens cast using M_5 were not cured at all, while for M_6 curing was undertaken for 5 days. M_7 and M_8 have the lowest w/c ratio among all mixes and a higher proportion of cement and sand; low strength was achieved for these two mixes through the use of AE agent and no curing. Since, the C:S:A ratio of 1:2:4 is the most commonly used ratio in NERC sites, mix M_3 is used again in M_9 and M_{10} with better curing in M_{10}. In addition to the use of normal aggregates in mixes M_1 to

M_{10}, recycled aggregates were used in mix M_{11} and M_{12} along with an AE agent. M_{13} had the same C:S:A proportions as M_7, but was cured for 5 days.

Early termination of curing is expected to reduce the target compressive strength at 28 days. If curing is terminated after 3 days, the strength is estimated to be reduced to 75% of the 28 days target strength (which can be achieved by undertaking continuous curing) [19]. AE is generally used to improve the concrete's freezing and thawing resistance; however, using a large percentage of AE agent introduces too much air and reduces strength. Excessive volume of voids through entrapped air or bleeding is a common problem in LSC. There is approximately 5% reduction in concrete strength for every 1% increase in entrained air [19]. In most mixes, the aggregates used comprised 50% of 20mm and 50% of 10mm river aggregates. Recycled demolition aggregates of the same size and proportion were used in two mixes to introduce inferior quality aggregates. In all mixes, Ordinary Portland Cement (OPC) type CEM II/A-L (32.5N) was used which includes 80% of the clinker content (A means higher clinker content up to 94%) and 20% of limestone (L). Its normal early strength (N) at 7 days is ≥ 16MPa and the standard strength at 28 days is 32.5MPa.

2.1.2 Specimen preparation

All mixes were batched and prepared in the laboratory. The mixes were placed in Ø100x 200mm steel cylinders and de-moulded the next day. The curing details are given in Table 1.

2.2 Test setup and instrumentation

For each concrete mix, a minimum of six specimens were tested in compression. The top cylinder surface was ground, and to further reduce the possible effect of confinement that may occur due to the friction between the steel platens and the ends of the specimens, a piece of Teflon sheet was placed between the platens and specimen ends as shown in Fig. 1. The specimens generally failed by vertical splitting (Fig. 1).

Fig. 1 Compression test of a Ø100x 200mm concrete cylinder exhibiting vertical splitting failure

A servo-controlled universal testing machine was used to undertake the compressive testing of the concrete cylinders. It is noted that, in order to record more accurately the post-peak response of the LSC, the tests were undertaken in displacement control (at a rate of 0.5mm/min). The compressive strain was measured according to BS 1881-121 [20] by using a device, which comprises two metallic rings and three Linear Variable Differential Transducers (LVDT), as shown in Fig. 2. Spring loaded clamp screws were used to mount in parallel (100 mm apart) the rings around the concrete specimen; the LVDTs are placed within the ring (Fig. 2b), at equal distances at an angle of 120 degrees.

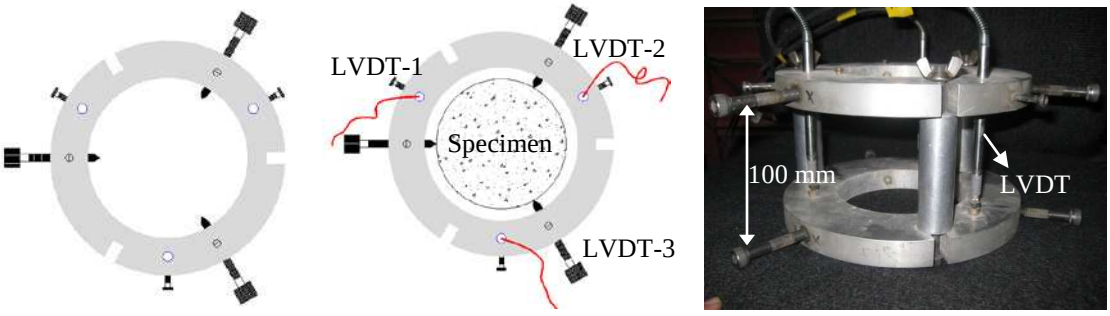

a) b) c)

Fig. 2 a and b Schematic diagram of ring assembly with LVDT's c) ring assembly with LVDT's by maintaining a 100mm gauge length

3 Test results

3.1 Compression

Table 2 shows the mean (μ), the standard deviation (σ) and coefficient of variation (C.O.V) of the cylinder compressive strength of all the LSC mixes developed in this study. The full details and results of the experiments are given in Ahmad [21]. Results from four different LSC mixes are given in Fig. 3. These σ-ε curves are the mean curves from the 3 LVDTs and the legend in each figure shows the number of each specimen from a mix.

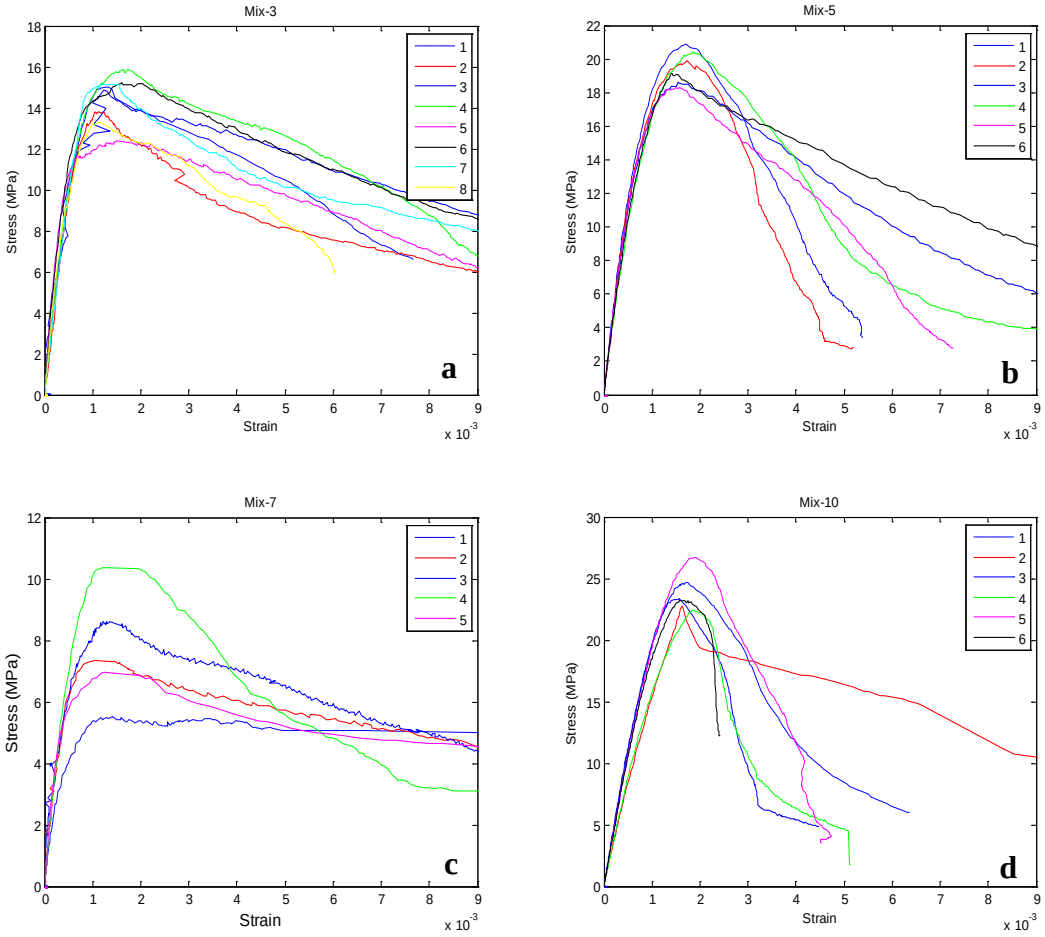

Fig. 3 Compressive stress-strain results for specimens of different mixes a) Mix 3 b) Mix 5 c) Mix 7 d) Mix 10

Table 2 Statistical details of the compression testing

MIX	f_{cmax},μ (MPa)	$f_{cmax,}\sigma$ (MPa)	C.O.V
M_1	7.8	1.83	0.240
M_2	5.9	0.95	0.160
M_3	14.5	1.18	0.082
M_4	14.4	2.47	0.170
M_5	19.5	1.02	0.052
M_6	26.5	1.89	0.071
M_7	11.2	0.86	0.077
M_8	11.4	0.81	0.071
M_9	17.8	1.10	0.100
M_{10}	23.9	1.59	0.070
M_{11}	10.1	1.90	0.200
M_{12}	15.3	1.60	0.100
M_{13}	16.2	2.60	1.600

3.2 Modulus of Elasticity of LSC

The modulus of elasticity (E_c) was evaluated from the experimental results by using the secant modulus (E_{sec}) in accordance with Eurocode-2 [10]. The E_{sec} value is largely dependent on the selection of the stress value and can include nonlinearity. Here, E_{sec} is evaluated by taking the slope between the origin and a stress, f_1, equal to 40% of the maximum concrete strength (f_{cmax}).

E_{peak} is also calculated by using f_{cmax} and the corresponding strain ε_{cmax}. The ratio of E_{sec} to E_{peak} is used in some σ-ε models as a material parameter which controls the degradation rate of the curve, in particular for the descending branch. Table A.1 of Appendix A shows the E_{chord}, E_{sec}, E_{peak} data for each specimen from the mixes tested at UoS. The statistical distribution of these data, including the μ, σ and COV for each mix is also given in Table A.1.

Additional data were also gathered from the literature regarding E_c for concrete strengths ranging from 14 to 30 MPa, mostly from Turkey [22-23] but also from Iraq and Korea [24-25].

The majority of the UoS data fall in the range of concrete strength between 5 and 20 MPa. Most of the additional data were in the range of 20 to 30 MPa. These two sets of data can be examined separately or as one set, to assess the statistical variation between E_{sec} and $f_{cmax.}$ The linear prediction

curves obtained by linear regression are shown in Eq. (1) to Eq. (3) for the UoS data, the additional data, and the combined data set, respectively.

$E_c = 13715 + 442\ (f_{cmax})$ MPa $R^2=0.42$ (1)

$E_c = 13332 + 528\ (f_{cmax})$ MPa $R^2=0.48$ (2)

$E_c = 12645 + 539\ (f_{cmax})$ MPa $R^2=0.60$ (3)

The linear best fit for the combined set is shown in Fig. 4. Combining the data improves the correlation coefficient. The linear Eq. (3) could be used for the range of concrete strength of 5 to 30 MPa. However, most advanced codes of practice relate E_{sec} to f_{cmax} with a nonlinear power equation. The Eurocode-2 [10] uses the power of 0.3 ($f_c'^{0.3}$)whilst ACI 318 [26] uses the power of 0.5 ($f_c'^{0.5}$).

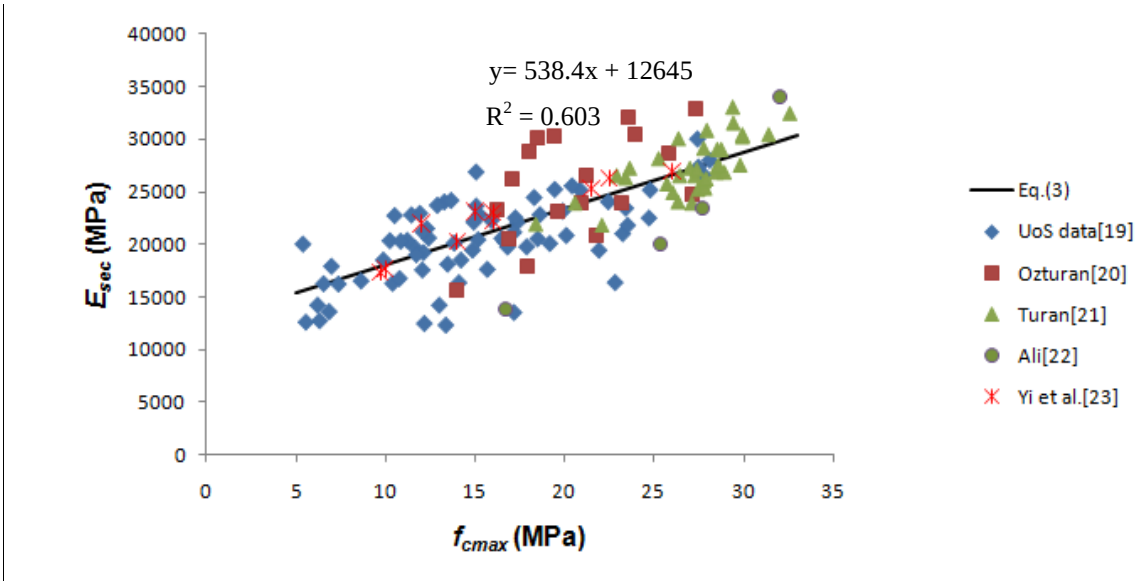

Fig. 4 E_c versus f_{cmax} (linear fit)

For nonlinear regression analysis, the power function in Eq. (4) was used, where the values of parameters α and β need to be determined.

$E_c = \alpha\ (f_{cmax}/10)^{\beta}$ GPa (4)

The nonlinear curve derived using nonlinear regression analysis involves an iterative process using the least square method. The nonlinear fit is shown in Fig. 5 alongside the 95% upper and lower prediction intervals (U.PI and L.PI). These 95% prediction intervals define the zone where 95% of

all data points are expected to fall. The R^2 = 0.59 for the nonlinear fit is slightly lower than the linear fit. The nonlinear calibrated E_c expression for LSC is given in Eq. (5).

$$E_c=17.81(f_{cmax}/10)^{0.42} \text{ GPa} \qquad R^2=0.59 \qquad (5)$$

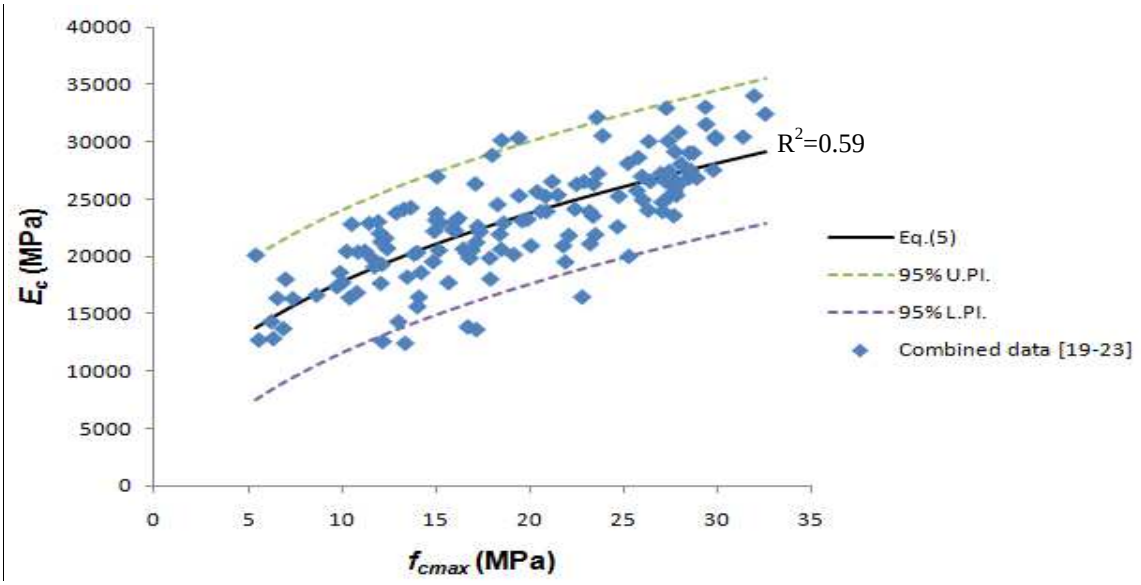

Fig. 5 E_c versus f_{cmax} (linear fit)

Eq. (5) is compared in Fig 6 with the predictions of other popular equations shown in Table 3. by ACI318 [26], Eurocode-2 [10], TS:500 [27], IS:456:2000 [28], and Mander et al [13].

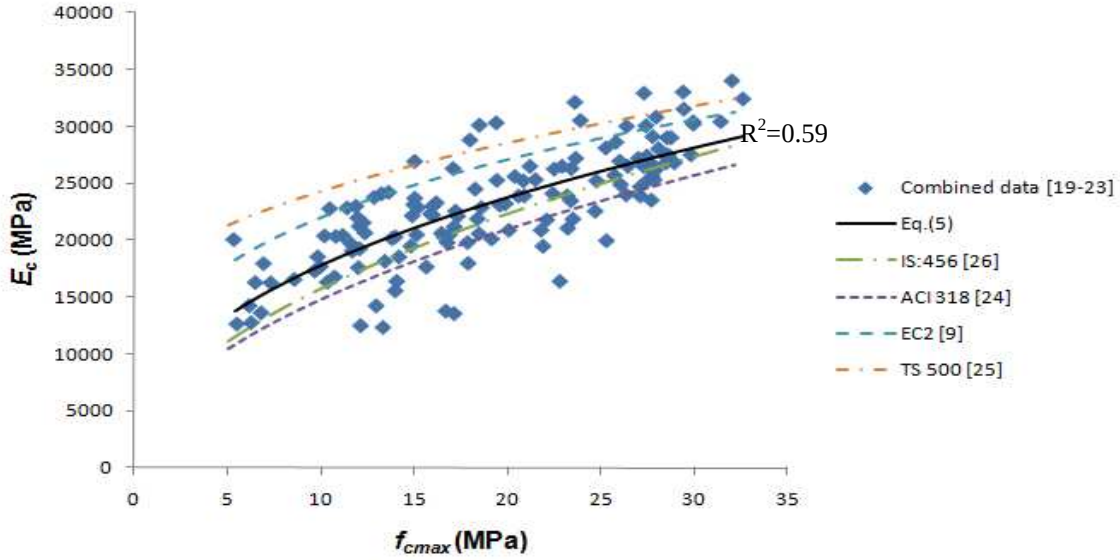

Fig. 6 Comparison of proposed nonlinear E_c equation with predictions of code equations

The comparison shows that the predictions from Eurocode-2 [10] and TS:500 [27] are un-conservative whilst the predictions from ACI 318[26] and IS:456:2000[28] are conservative. It is

interesting to note that the power factor in the LSC E_c nonlinear equation has a value of 0.42 which lies approximately in the middle of the power factor of the ACI 318 (0.5) and Eurocode-2 (0.3). Eq. (5) is adopted here for evaluating the value of E_c for LSC. The uncertainty factor of ±3110 MPa corresponding to ±1σ has been determined for Eq. (5) considering a normal probability density function for model prediction errors. This factor is an additional model uncertainty factor (besides the commonly used f_{cmax} uncertainty) and can be used in probabilistic analytical assessments.

Table 3 Different code equations for predicting E_c

Sr. no.	Code/Researcher	Expression for E_c	comments
1	ACI 318	$E_c = 4700\sqrt{f_c'}$, *MPa*	-
2	EC2 (2004)	$E_{cm} = 22\left(\frac{f_{cm}}{10}\right)^{0.3}$ *GPa*	-
3	Turkish code (TS:500)	$E_c = 3.25\sqrt{f_c'} + 14$ *GPa*	-
4	Indian code (IS:456:2000)/Mander(1988)	$E_c = 5000\sqrt{f_c'}$ *MPa*	IS:456:2000 ±20%.of the calculated values

3.3 Peak strain (ε_{cmax})

The peak strain ε_{cmax} values corresponding to f_{cmax} for each specimen from different mixes are given in Table A.2 along with the statistical characteristics for each mix. The data were fitted with linear and nonlinear curves to find the most suitable relationship between ε_{cmax} and f_{cmax}. Besides the UoS data, data from experimental work undertaken in Pakistan at UET[18] are also included in the analysis. The linear fit on the UoS data scatter is shown in Fig. 7 and the linear equation, used to evaluate ε_{cmax}, is given in Eq. (6).

$$\varepsilon_{cmax} = 0.00003 f_{cmax} + 0.001 \qquad R^2 = 0.49 \qquad (6)$$

It can be seen from Fig. 7 that ε_{cmax} lies between 0.001 to 0.0017 for the majority of specimens having f_{cmax} between 5 and 15 MPa. For f_{cmax} 33.3MPa the value of ε_{cmax} predicted by Eq. (6) reaches 0.002 and beyond that it is normally considered constant. The ε_{cmax} values adopted by different codes are 0.002 for Eurocode-2[10], 0.0022 for the FIP-CEB model code 90 [9] and for ACI318[26] values between 0.0015 and 0.002. Though the common approach of assuming constant

strain at all strength levels is quite convenient, it is not confirmed experimentally for LSC and lower values should be used.

The linear fit of Eq.(6) is also compared with existing linear peak strain relations by Carreira and Chu [8] and Ros [29], as shown in Fig. 7.

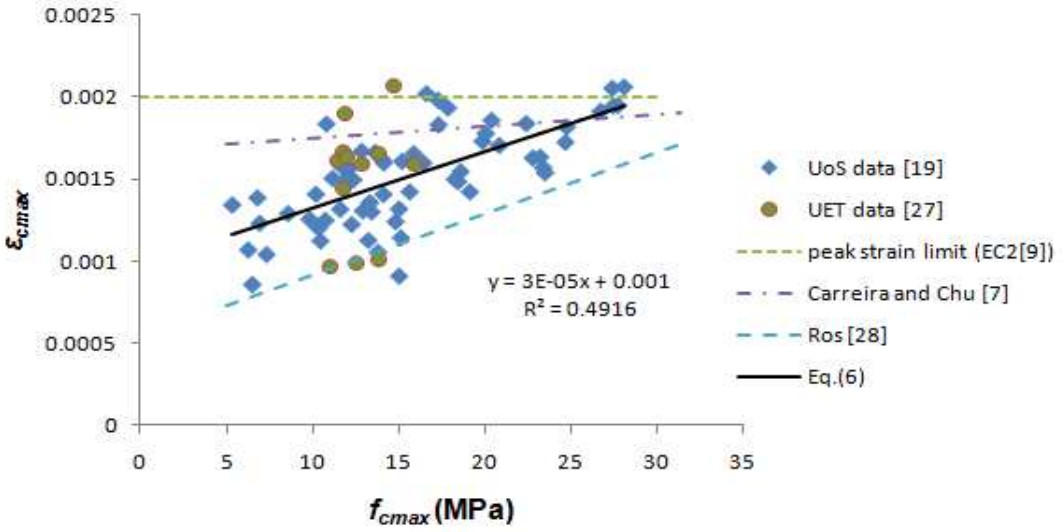

Fig. 7 f_{cmax} vs ε_{cmax} scatter for combined UoS and UET data with linear fit.

The relation by Carreira and Chu [8] predicts higher strains in the LSC region and achieves the code based ε_{cmax} value at higher f_{cmax}, whereas the relation by Ros [29] under-predicts the strains at all the concrete strength ranges and also attains the code based ε_{cmax} at relatively higher f_{cmax} values.

To find the best nonlinear fit for the data, the Popovics [30] function given in Eq.(7) was adopted and the nonlinear fit along with the 95% upper and lower prediction intervals are plotted in Fig. 8 by using Eq.(8).

$$\varepsilon_{cmax} = \alpha(f_{cmax})^b \qquad (7)$$

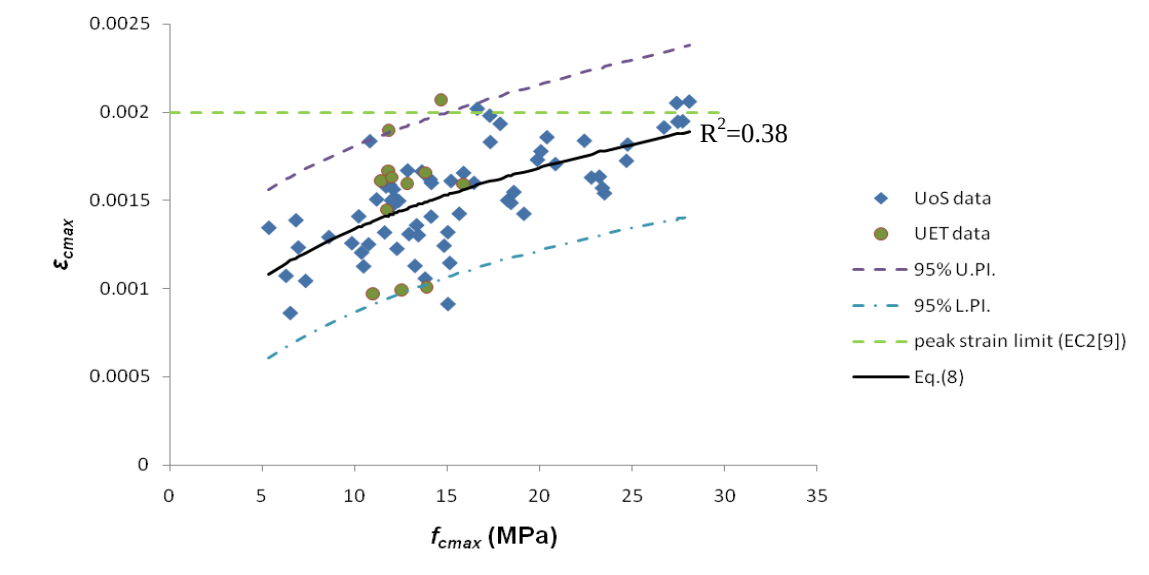

Fig. 8 f_{cmax} vs ε_{cmax} scatter for combined UoS and UET data with non-linear fit

The nonlinear expression obtained is given by Eq. (8).

$$\varepsilon_{cmax} = 0.00061(f_{cmax})^{0.33} \qquad R^2=0.38 \qquad (8)$$

A comparison between nonlinear ε_{cmax} relations by Popovics [30], Saenz [31] and Eq.(8) is made in Fig. 9.

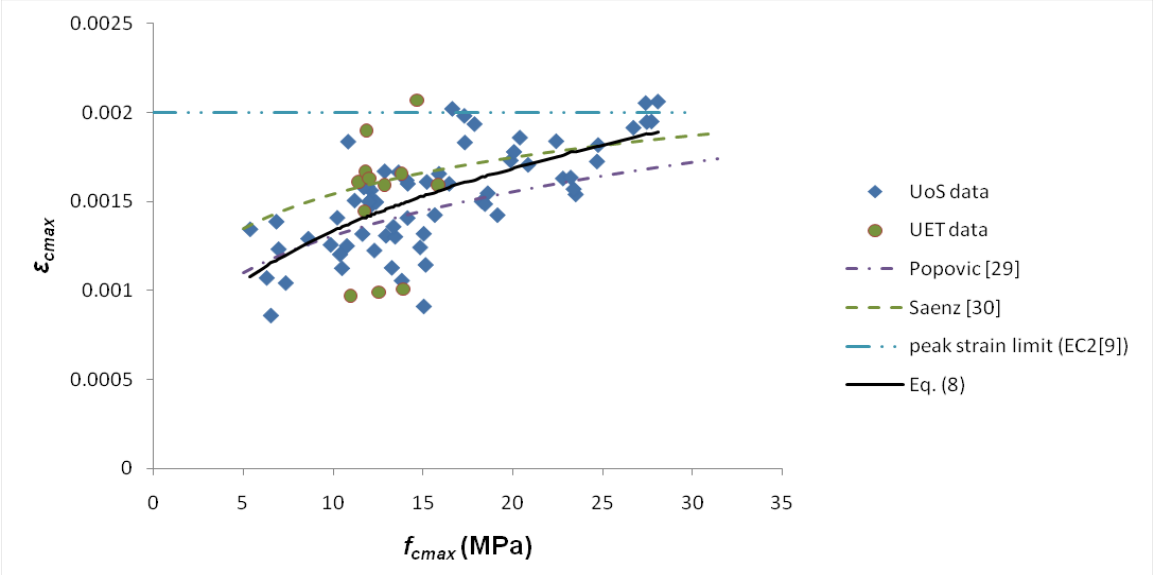

Fig. 9 Comparison between existing ε_{cmax} relations and the nonlinear fit

The comparison shows that the Popovics [14] relation slightly over estimates ε_{cmax} in the f_{cmax} range of 5 to 8 MPa but underestimates ε_{cmax} as f_{cmax} increases. The ε_{cmax} predictions by Saenz [31] are

high for f_{cmax} up to 22 MPa. In general, Eq. (8) is in good agreement with these two equations. However, the R^2 value for the linear fit is better than the nonlinear fit, hence the proposed linear ε_{cmax} relationship will be used for defining the σ-ε behaviour of LSC. An uncertainty factor of ±0.00021 corresponding to ±1σ was evaluated for the linear model in Eq. (6) which can be used to evaluate maximum and minimum values.

3.4 Ultimate strain ($\varepsilon_{c,ult}$)

The value of $\varepsilon_{c,ult}$ is generally taken as ε_{c85} which is the strain corresponding to f_{c85} (stress at 85% of the f_{cmax}). The f_{cmax} versus ε_{c85} results along with the linear fit of Eq. (9) are shown in Fig. 10.

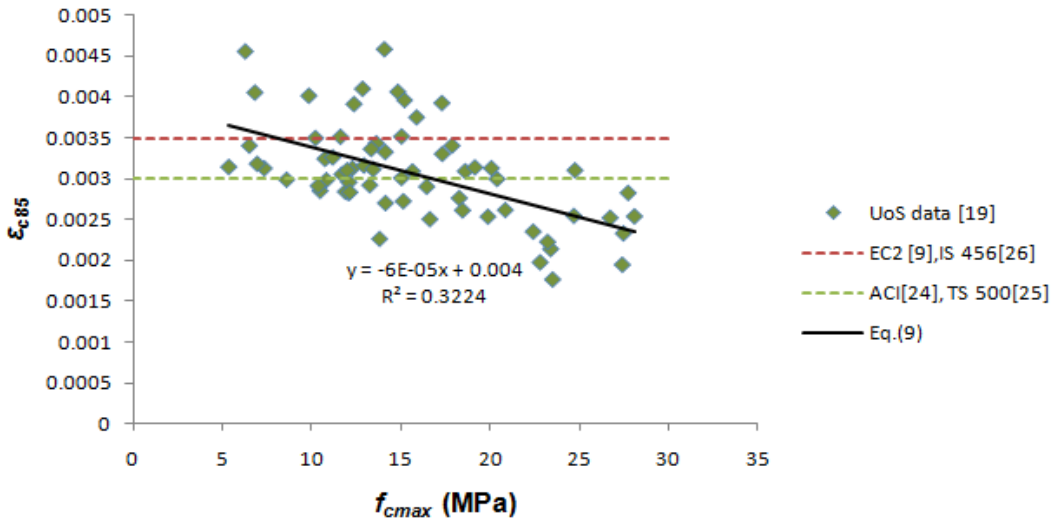

Fig. 10 f_{cmax} vs ε_{c85} scatter for LSC specimens with linear fit

$$\varepsilon_{c85} = -0.00006 f_{cmax} + 0.004 \qquad R^2 = 0.32 \qquad (9)$$

Eurocode-2 and ACI suggest constant values of 0.0035 and 0.003, respectively for $\varepsilon_{c,ult}$ values which differ slightly from the observed trend of ε_{c85} which shows that LSC specimens between 5 and 15 MPa can achieve higher failure strains. However, for concrete strengths 15 to 25 MPa, ε_{c85} falls below the code values. Nonetheless, it should be noted that there is a lack of data for that particular strength range in the current study to arrive at any firm conclusions and change the current practice. To evaluate the value of $\varepsilon_{c,ult}$ and value of stress at failure, it is important to know when the mean stress curve, intersects the experimental σ-ε curve as shown in Fig. 11. Beyond this strain an RC

flexural element designed to code provision will not be able to carry further load and fail. The mean stress factor α was calculated at each increment with respect to stress (f_{ci} and strain ε_{ci} using Eq. (10) which is then used for calculating the mean stress (f_{cmean}) at each step using Eq. (11).

$$\alpha_i = \int_0^{\varepsilon_{c,n}} f_c d\varepsilon_c \Big/ f_{ci}\varepsilon_{ci} \tag{10}$$

$$f_{cmean,}i = \alpha_i f_{ci} \tag{11}$$

When f_{cmean} curve intersects the experimental σ-ε curve, that value of $f_{cmean,i}$ and the corresponding strain are noted. These correspond to the ultimate stress $f_{c,ult}$ and ultimate strain $\varepsilon_{c,ult}$. For LSC the intersection of these two curves generally occurred beyond f_{c85}. An example of evaluating $f_{c,ult}$ and $\varepsilon_{c,ult}$ using this process is shown in Fig. 11.

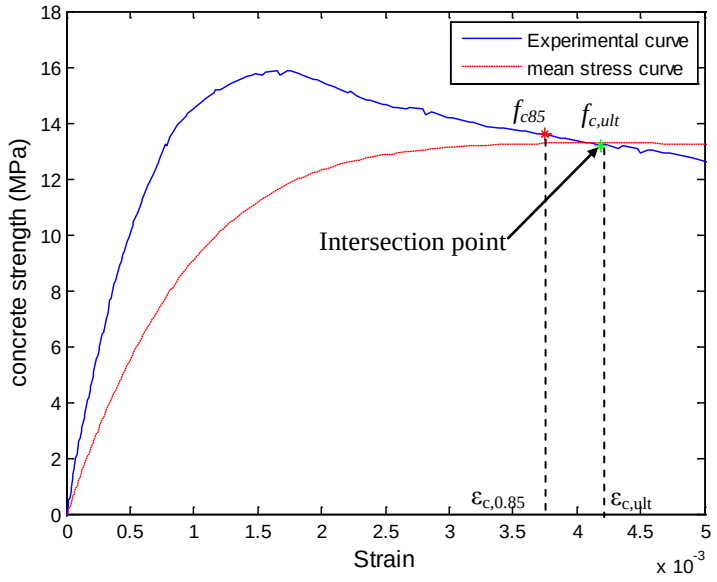

Fig. 11 Comparison between the experimental and the mean stress-strain curve

The statistics of $f_{c,ult}$ and corresponding strain $\varepsilon_{c,ult}$ are given in Table A.2. The $\varepsilon_{c,ult}$ versus f_{cmax} and $\varepsilon_{c,ult}$ versus $f_{c,ult}$ scatter points for all the specimens along with the linear fit of Eq. (12) and Eq. (13) are shown in Fig. 12 and 13, respectively.

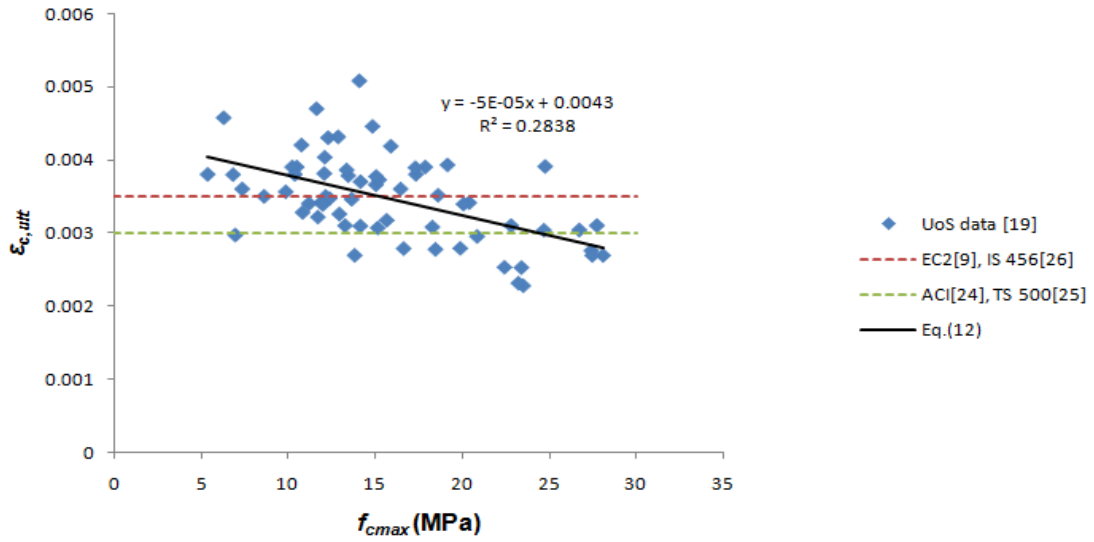

Fig. 12 f_{cmax} versus $\varepsilon_{c,ult}$ scatter for LSC specimens with linear fit

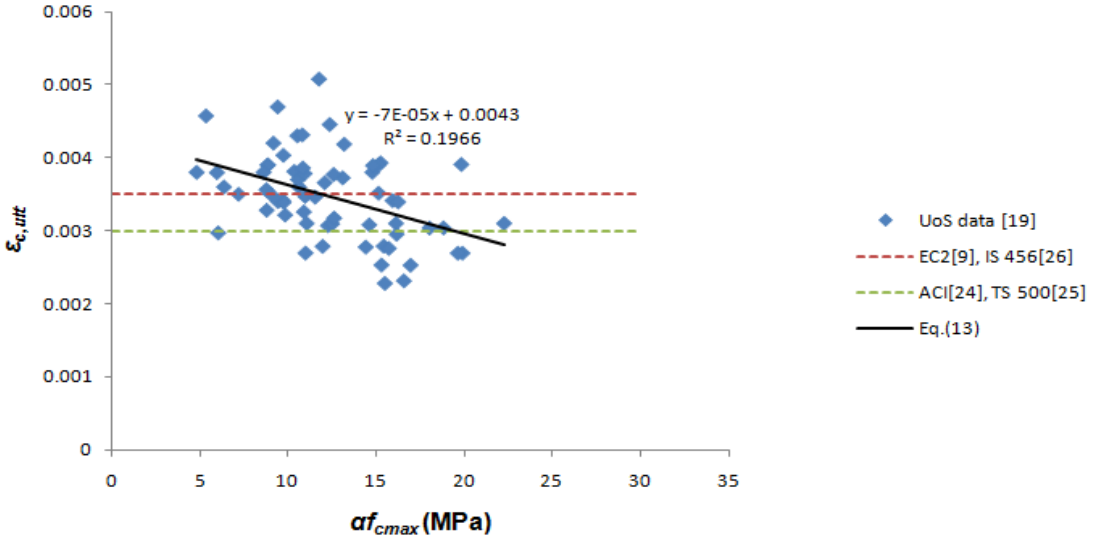

Fig. 13 $f_{c,ult}$ versus $\varepsilon_{c,ult}$ scatter for LSC specimens with linear fit

$$\varepsilon_{c,ult} = -0.00005 f_{cmax} + 0.004 \qquad R^2 = 0.28 \qquad (12)$$

$$\varepsilon_{c,ult} = -0.00007 f_{c,ult} + 0.004 \qquad R^2 = 0.20 \qquad (13)$$

The $\varepsilon_{c,ult}$ point on the degrading branch is often called an "inflection" point. This point is used in many concrete σ-ε models for controlling the degrading branch gradient. Not many relationships can be found in the literature to evaluate the inflection point because of the complex degrading behaviour of the descending branch.

Wee et al.[32] proposed Eq. (14) for finding the inflection point.

$$\varepsilon_{c,ult} = (510\text{-}f_{cmax})10^{-5} \quad (14)$$

Another relationship given in Eq. (15) for $\varepsilon_{c,ult}$ was developed by Dahl[33];

$$\varepsilon_{c,ult}/\varepsilon_{c'} = 2.5\text{-}0.3\ln(f'_c) \quad (15)$$

The predictions of the Eq. (14) and (15) are compared with the $\varepsilon_{c,ult}$ scatter and are shown in Fig. 14.

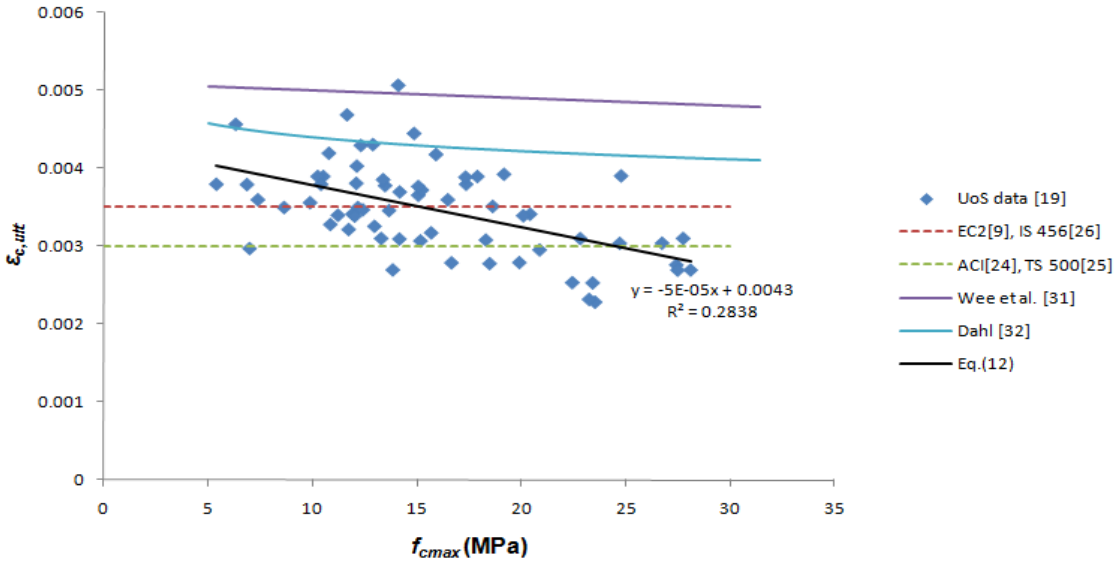

Fig. 14 Comparison of $\varepsilon_{c,ult}$ scatter with the inflection point strain prediction

The predictions by these two models are un-conservative, hence, the linear fit expression of Eq. (12) will be used in the current study. An uncertainty factor of ±0.000692 corresponding to ±1σ will be used.

The values of $\alpha = f_{c,ult}/f_{cmax}$ obtained from the analysis (Fig. 11) of individual specimen σ-ε data are plotted in Fig. 15. The mean value of α is calculated to be 0.80 (this is usually taken as 0.85 by various codes). The lower value of α is due to the lower $f_{c,ult}$ value as compare to the f_{c85} (Fig. 11) for most of the tested specimens. This indicates a lower compressive stress at failure for LSC structural elements.

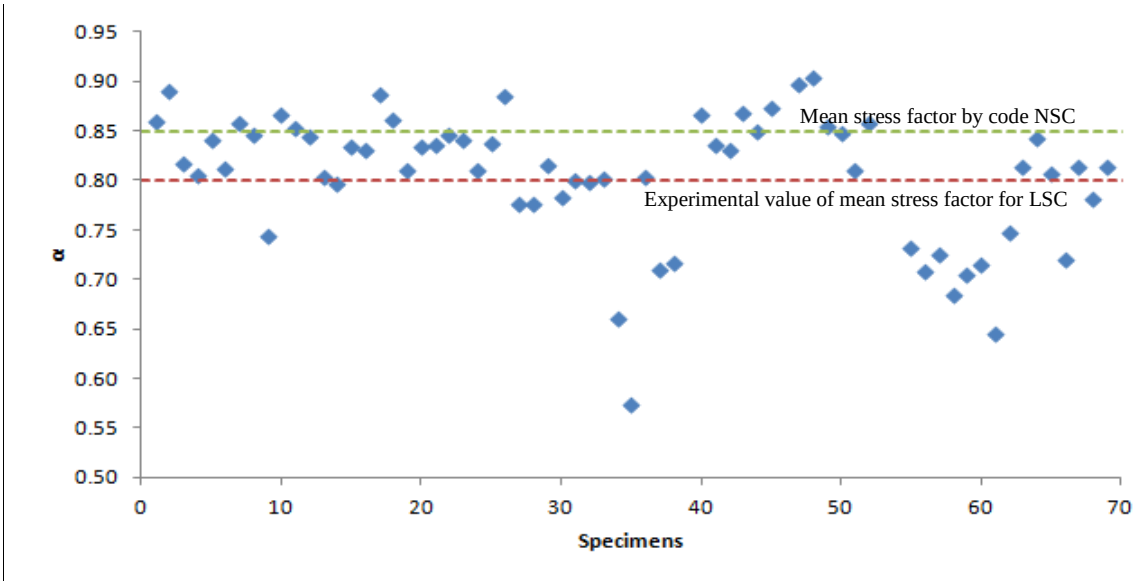

Fig. 15 Plot showing α for various strength specimens

4 Modelling the compressive stress-strain (σ-ε) behaviour of LSC

Different σ-ε relationships can be found in the literature for unconfined NSC and HSC subjected to uni-axial compressive loading [8-11, 13-14]. Researchers often try to use various hypotheses and approaches to accommodate the effect of multiple factors (aggregate types, cement types, aggregate gradation, testing conditions and strength ranges). However, all analytical σ-ε relationships are developed primarily on a curve fitting basis, and aim to satisfy different boundary conditions such as

1- σ-ε curve slope at origin, $df_c/d\varepsilon_c = E_c$ and $\varepsilon_c=0$

2- maximum strength point, $f_c=f_{cmax}$; $df_c/d\varepsilon_c = 0$, $f_c=f_{cmax}$; $\varepsilon_c = \varepsilon_{cmax}$

3- Inflection point, $f_c=f_i$; $\varepsilon_c = \varepsilon_{ci}$ (where ε_{ci} is $\varepsilon_{c,ult}$)

Additional boundary conditions may be used for the ascending branch at the location of $0.4f_{cmax}$ and for the descending branch to capture the residual strength f_{resd} at a certain strain level. These boundary condition are;

4- At the elastic limit point $f_c=0.4f_{cmax}$; $\varepsilon_c = \varepsilon_{c,0.40}$

5- Residual point $f_{resd} = 0$ when $\varepsilon_c = \infty$

Since, various mathematical formulations in the literature fulfil satisfactorily the requirements of the boundary conditions, the general trend is to use these existing σ-ε formulations to achieve the best fit with the experimental data. Hence, it is important to choose a formulation which is compact (single equation), satisfies all the essential boundary conditions and correlates well with the LSC σ-ε experimental data especially the degrading branch. For this purpose, a variety of σ-ε formulations for unconfined concrete are examined.

4.1 Assessment of existing σ-ε relations

Using the newly developed LSC expressions for E_c (Eq.(5)), ε_{cmax} (Eq.(6)) and $\varepsilon_{c,ult}$ (Eq.(12)), the predictions of the existing well known and relevant concrete σ-ε models are compared with the experimental data. Some of the representative plots showing the performance of these models in comparison with the LSC mean experimental σ-ε results are given in Fig. 16. A typical LSC range from 10 to 15 MPa is selected for NERC structures, whilst a normal strength concrete range from25 to 30 MPa is selected for comparison purposes.

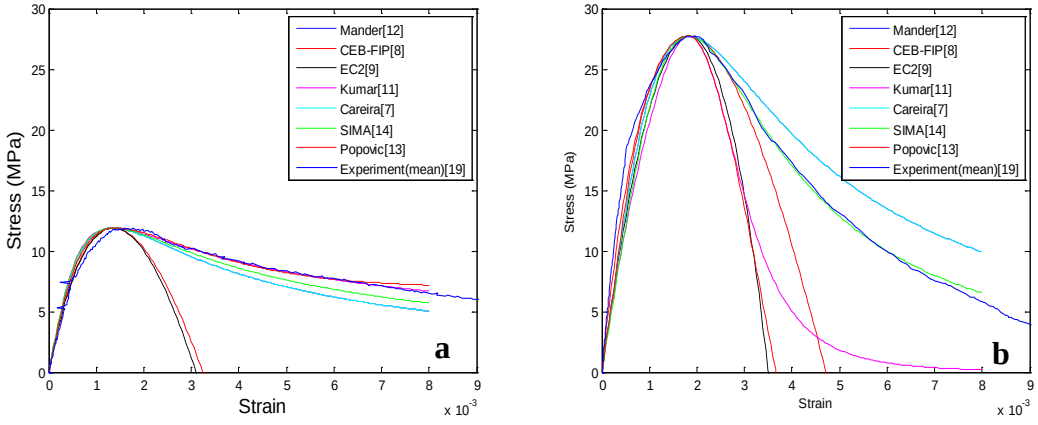

Fig. 16 a and b Comparison of the predictions of different σ-ε relations with mean experimental data

The different σ-ε relations examined are described in the following sub-sections.

4.1.1 Popovic (1973) and Mander (1988)

Popovic [14] proposed a model for unconfined concrete as given by Eq.(16)

$$f_c = f'_c \, (\varepsilon_c/\varepsilon_o) \, n/(n-1+(\varepsilon/\varepsilon_o)) \qquad (16)$$

Where;

$n=0.0004f'_c+1$ (f'_c in psi) for the concrete (17)

This model predicts the LSC degrading behaviour better than Eurcode2 (2004) and CEB-FIP model code 90 models (Fig. 16 a and b) and the material parameter 'n' evaluated from Eq. (17) is capable of controlling the descending branch to a certain level.

Since, the performance of the Popovics model is better for LSC as compared to the other examined models, models based on Popovics formulations require further investigation.

The following Eq.(18) describes the Mander model [13] for concrete and adopts the expression similar to [14] but instead of the 'n' factor, it uses 'r' which increases with stiffness degradation.

$f_c= f'_c\, x\, r / r-1+x^r$ (18)

Where;

$x= \varepsilon_c/\varepsilon'_c$, $r=E_c/E_c-E_{sec}$ (19)

$E_c=5000\sqrt{f'_c}$, $E_{sec} = f'_c/\varepsilon'_c$ (20)

E_{sec} = secant modulus of concrete corresponding to f'_c

ε'_c = peak strain of unconfined concrete

The model by Carreira and Chu[8] (shown in Fig. 16 a and b) also results in exactly the same behaviour as the model by Mander et al[13].

4.1.2 Eurocode-2(2004) and CEB-FIP MC90

Since Eurocode-2 [10] considers a constant strain value for ε_{c1}, the degrading branch starts after this strain is achieved. In the case of LSC, especially in the range of 5 to 15 MPa the maximum strains vary from 0.001 to 0.0017 (Fig. 7) which means the degrading branch starts earlier and descents to zero at a lower strain (see Fig. 16a and b). Hence, the earlier descent of the Eurocode-2 model in the degrading branch makes it unsuitable for use in this study. It should be noted that this model showed better agreement with the experimental results for the concrete strength range between 25 and 30

MPa. Similar to Eurocode-2, in the CEB-FIP model code 90 [9] relationship, the peak strain is constant and the degradation branch is steep, hence, it is also unsuitable for LSC.

4.1.3 Kumar (2004) and Sima et al (2007)

The sophisticated mathematical formulation by Kumar[12] can be used for a wide range of concrete strengths and does not require any modification factors. According to this model, there is no fixed location for failure on the degrading branch and failure may be defined by the general point, a point close to the inflection point, the residual point or any point in between. When calibrated, this model gives a good fit especially of the degrading curve of LSC in the strength range between 5 to 15 MPa (see Fig. 16).

The σ-ε formulation by Sima et al [15] which involves different equations for three different branches is also examined. In this model an exponential function is used after the elastic limit to model damage. As compared to the Kumar model, an extra boundary condition is included for the elastic limit of the concrete and an inflection point is also required. This model gives very close results to Kumar model predictions.

4.1.4 Conclusion on formulations

From the comparison of all the models, shown in Fig. 16 a and b, it can be concluded that the formulations by Kumar and Sima predict the σ-ε behaviour of LSC better than other models. These formulations are particularly good in the strength range of 10 to 15 MPa. With increasing in strength, these models also give reasonable results, however, the code models, like Eurocode-2, become more suitable for concrete strength above 25MPa and NSC.

Although Kumar and Sima formulations give good results, the equations are complex and are unlikely to be adopted for general use. Since the main concern in deriving a good model is the degrading behaviour, a comparative analysis is carried out between the simple and well known model of Mander et al[13] and the more sophisticated model of Kumar by considering $f_{c,ult}$ as the key parameter. The analysis details are given in the following section.

5 Degrading branch of the σ-ε curve for LSC

In this analysis $f_{c,ult}$ is determined using the Mander and Kumar models corresponding to the experimental values of $\varepsilon_{c,ult}$. The predicted strength values for each specimen in different groups are evaluated and normalized with respect to the experimental $f_{c,ult}$ to evaluate the difference between the model predictions and experiments. The results of $f_{c,ult,Mander}/f_{c,ult}$ vs f_{cmax} and $f_{c,ult,Kumar}/f_{c,ult}$ versus f_{cmax} are shown in Fig. 17 and 18, respectively.

From these plots, a contrasting trend is seen between the two predictions at different strength ranges. The predictions from Mander et al were in general found to be less than 1 (underpredicted) between concrete strengths of 5 and 15 MPa, and the majority of results are more than 1 (overpredicted) between 15 and 30 MPa. Whereas normalized predictions from Kumar were in general found to be more than or close to 1 between 5 and 15 MPa, but the majority of the results are less than 1 between 15 and 30 MPa. The μ and σ of normalized predictions using Mander model are 0.96 and 0.18, respectively. For Kumar model these values are equal to 0.95 and 0.15. The difference between the μ and σ of the predictions from two models is not so significant.

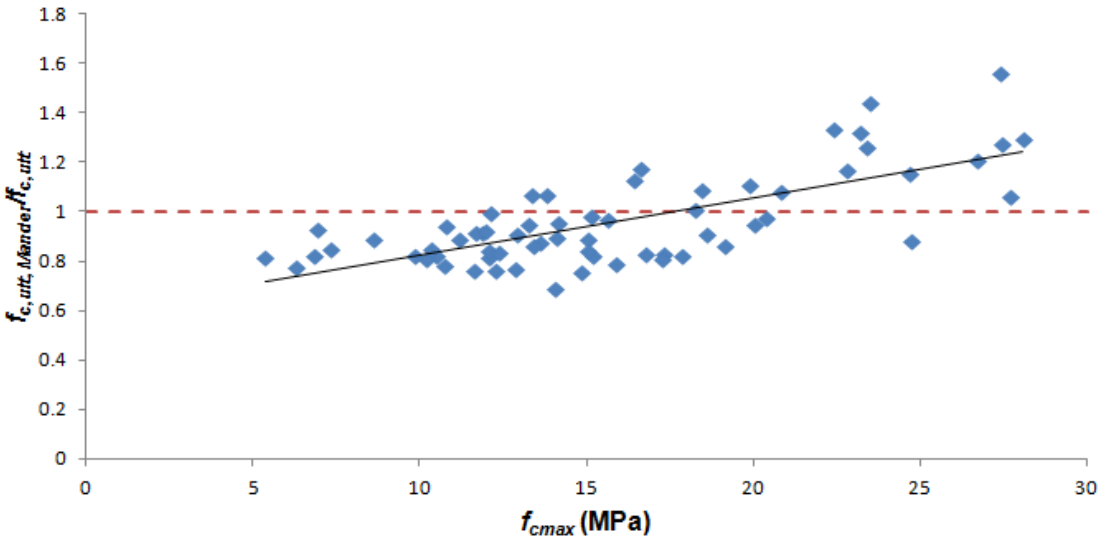

Fig. 17 Scatter of the $f_{c,ult,Mander}$ normalized with respect to the experimental $f_{c,ult}$

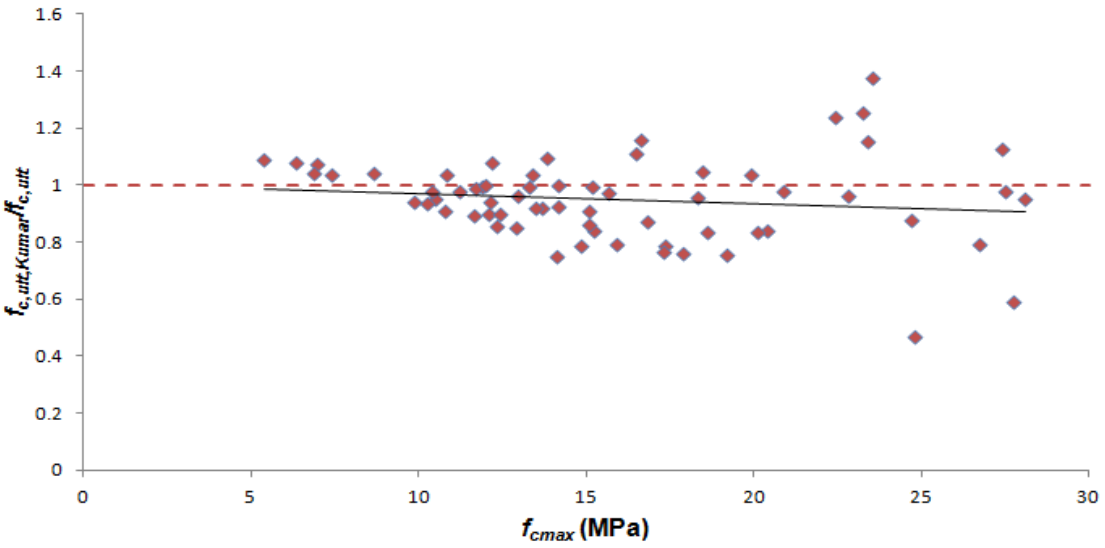

Fig. 18 Scatter of the $f_{c,ult,Kumar}$ normalized with respect to the experimental $f_{c,ult}$

The Kumar model is much more complex compared to the Mander model due to its lengthy equations and because of the iterative process involved for evaluating the parameter 'n'. On the other hand, the Mander model is simple and has been used by many researchers [34-36] in the assessment of NSC RC structures. This model is applicable to all section shapes and all levels of confinement. To avoid the complexity related with the Kumar model and to improve the Mander model for defining the σ-ε behaviour of LSC, a modification factor is introduced to the parameter 'r' in Eq. (20) to control the slope of the descending branch. The resulting equation is given by Eq. (21). The main purpose of introducing the modification factor is to reduce the underprediction of the descending branch and bring it closer to the experiments by maintaining an acceptable mean for $f_{c,ult,Mander} / f_{c,ult}$. This modification factor 'β' is introduced and calibrated through an iterative process in which the main condition is to normalize the scatter trend in Fig. 17 and to maintain a mean of $f_{c,ult,Mander} / f_{c,ult}$ up to 1.0. The selected modification factor to be used in the modified Mander model for LSC is given in Eq. (22).

$$f_c = f'_c \, x \, r \, / \, r-1+x^{r\beta} \qquad \text{(MPa)} \qquad (21)$$

$$\beta = ((f'_c+23)/38)^{0.45} \qquad f'_c \text{ in MPa} \qquad (22)$$

Fig. 19 shows the normalized predictions from the modified Mander model.

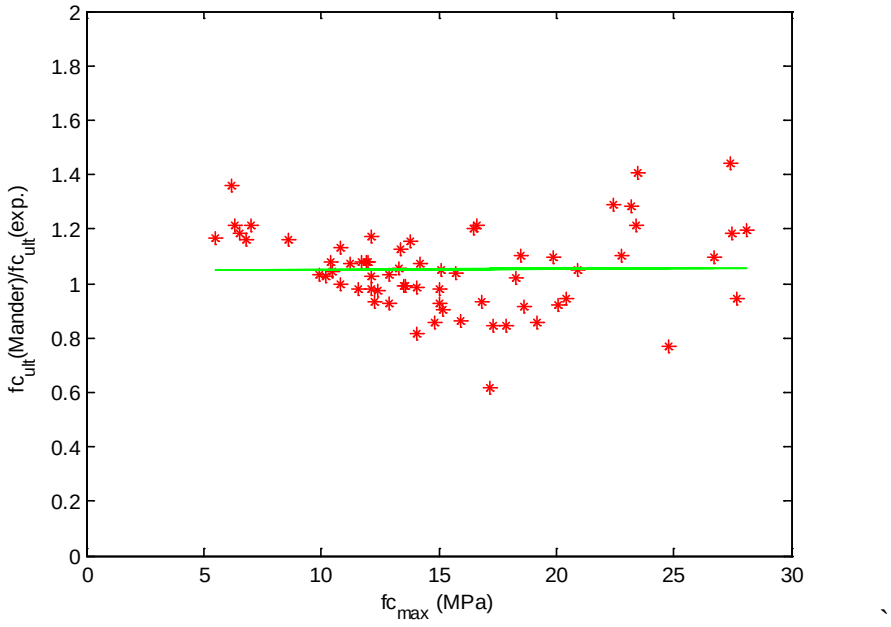

Fig. 19 Scatter of the $f_{c,ult,modified\ Mander}$ normalized with respect to the experimental $f_{c,ult}$

A comparison is made between the modified Mander model predictions and mean experimental σ-ε results for different LSC ranges as shown in Fig. 20 and Fig. 21. Other relevant model predictions are also included in the comparison.

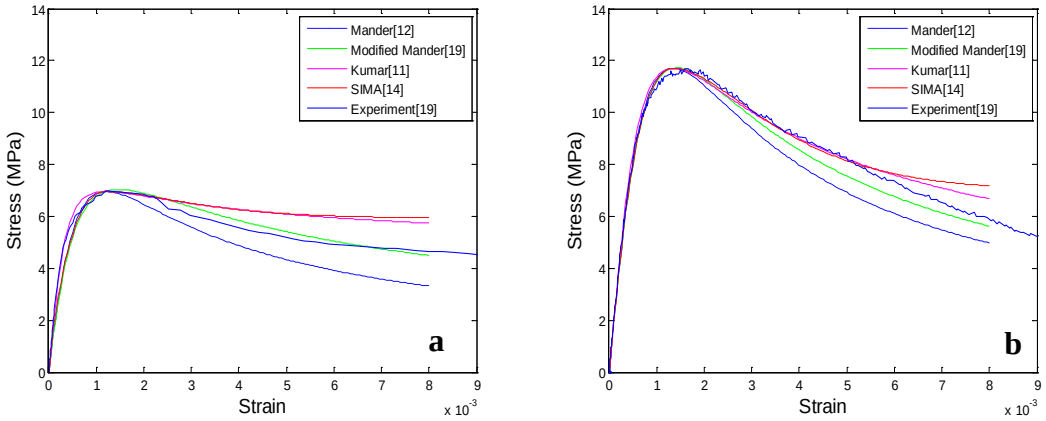

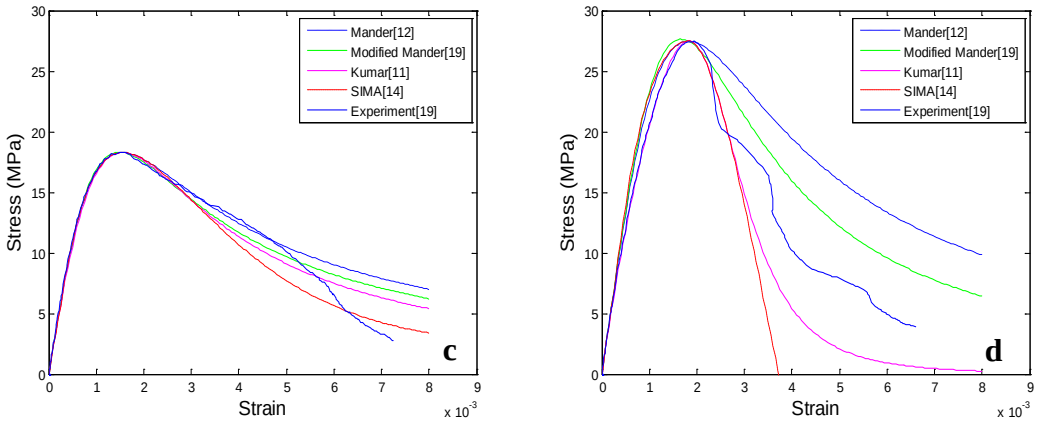

Fig. 20 a, b, c and d. Comparison of mean experimental σ-ε results with different existing and LSC model predictions

It is found from the comparisons that for extremely low strength concretes, such as between 5 and 10 MPa, the Mander model without modification does not predict very well the decrease in the steepness of the degrading branch (Fig. 20a). The Kumar and Sima models predict the descending branch very well in this strength range, however, the Kumar model could not predict very well the σ-ε up to ε_{cmax} for concrete strength between 5 and 6 MPa, as shown in Fig. 21. The modified Mander model predictions are in close agreement with the experiments in extremely low concrete strength between 5 and 10 MPa, as shown in Fig. 20a and 21.

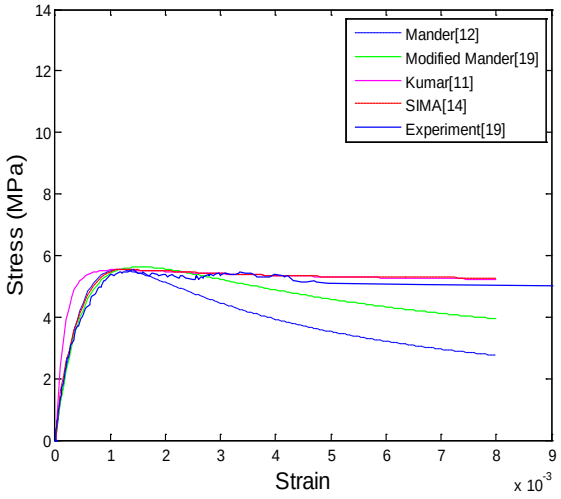

Fig. 21 Comparison of extremely LSC experimental σ-ε curve with the models prediction

For the strength range 10 and 15 MPa (Fig. 20b), the modified Mander, Kumar and Sima models are in close agreement with the experimental outcome in predicting the descending branch behaviour. The Mander model without modification under predicts the behaviour of the degrading σ-ε branch. For NSC around 25 to 30 MPa, the trend is found to be reversed as the Mander model without modification starts over predicting the behaviour of the degrading σ-ε branch in this concrete strength range. The modified Mander model prediction is found to be slightly higher than other models (Kumar and Sima) which under predicted the degrading behaviour for NSC.

The original Mander model predictions are close to the experiments and other model predictions in the concrete strength range 10 to 20MPa as shown in Fig. 20b and 20c.

The LSC σ-ε model established through the modification to the Mander model predicts better the degrading σ-ε branch of LSC as compared to the more sophisticated models and can be used in analytical vulnerability assessment of NERC structures.

6 Conclusions

LSC having different ranges of concrete strength (5 to 25MPa) was tested in compression at UoS to study the σ-ε characteristics. New E_c, ε_{cmax}, $\varepsilon_{c,ult}$ expressions are developed which are used to model the σ-ε behaviour of LSC. The power factor in the E_c nonlinear equation has a value of 0.42 which lies approximately in the middle of the power factor of the ACI 318 (0.5) and Eurocode-2 (0.3). The value of ε_{cmax} lies between 0.001 to 0.0017 for the majority of specimens for f_{cmax} between 5 and 15 MPa. For f_{cmax} greater than 15MPa, ε_{cmax} starts to increase and for f_{cmax} of around 30 MPa, the results from both linear and nonlinear equations reach the values given by the codes for NSC.

The ultimate strain $\varepsilon_{c,ult}$ is determined when the mean stress-strain curve intersects the experimental stress-strain curve. For the LSC specimens having f_{cmax} between 5 and 15 MPa, $\varepsilon_{c,ult}$ is above 0.004. However, the $\varepsilon_{c,ult}$ value for the specimens with concrete strength 15 to 25 MPa falls below 0.003. The mean value of α (mean stress factor) which is usually taken as 0.85 by different codes is calculated to be 0.80 for LSC. $\varepsilon_{c,ult}$ is found to be 13.1% higher than ε_{c85}.

The σ-ε models by Kumar[12] and Sima et al. [15] predict the σ-ε behaviour of LSC better than other models particularly for concrete strength between 5 and 15 MPa by using the new LSC modulus of elasticity and strain models. However, these models result in lengthy equations and are too complex for general use. Due to this reason, the Mander model was calibrated through a modification factor and is adopted due to its simplicity (Modified Mander Model for LSC). The derived LSC σ-ε model is particularly efficient at predicting concrete degrading behaviour between 5 and 10 MPa, however, between 15 and 20 MPa, the result of this model gets closer to the original Mander model. The LSC σ-ε model can be used in design or for the analytical vulnerability assessment of low strength RC structures.

Acknowlegement

The first author acknowledges the financial support provided by Higher Education Commission (HEC), Pakistan to conduct this research as a part of developing analytical seismic vulnerability assessment framework for reinforced concrete structures of developing countries.

Appendix A

Table A.1. Statistics of the different modulus of elasticity (E_{chord}, E_{sec}, E_{peak})

Mixes	f_{cmax} (MPa)	E_{chord} (MPa)	E_{sec} (MPa)	E_{peak} (MPa)	n
124_0.82-no curing					
M_1	5.5	11727	12677	3890	3.3
	7.4	14787	16286	7052	2.3
	8.6	11074	16584	6668	2.5
	10.4	15932	16359	8623	1.9
	7.0	16914	17976	5646	3.2
mean	7.8	14087	15976	6376	2.63
St.dn.	1.8	2576	1968	1754	0.58
COV	0.24	0.18	0.12	0.28	0.22
134_0.92-no curing					
M_2	6.3	13898	12806	5876	2.2
	6.8	12006	13671	4926	2.8
	6.2	11849	14282	4388	3.3
	5.4	20990	20079	3995	5.0
	6.5	20600	16323	7585	2.2
mean	6.2	15869	15432	5354	3.08
St.dn..	0.5	4571	2903	1433	1.18
COV	0.09	0.29	0.19	0.27	0.38
124_0.75-5 days curing (A)					
M_3	15.0	25503	26922	11397	2.4
	13.8	20402	20176	13080	1.5
	14.8	13022	19510	11941	1.6
	15.9	21981	22332	9596	2.3
	12.4	19308	20668	8271	2.5
	15.2	21617	22885	9450	2.4
	15.1	19690	20497	13230	1.5
	13.3	24010	24086	11757	2.0
mean	16.5	23648	25297	12675	2.34
St.dn..	1.2	3751	2475	1800	0.41
COV	0.07	0.16	0.10	0.14	0.18
134_0.75-5 days curing					
M_4	14.1	15990	16425	8696	1.9
	13.6	23001	24224	8197	3.0
	12.9	16971	23764	7706	3.1
	11.6	20644	19738	8821	2.2
	15.0	23304	23699	16506	1.4
mean	13.5	19982	21570	9985	2.3
St.dn.	1.3	3376	3399	3672	0.7
COV	0.10	0.17	0.16	0.37	0.30
133_no curing					
M_5	20.9	25429	25218	12221	2.04
	19.9	22315	23215	11489	2.02
	18.6	22313	22884	12024	1.90
	20.4	25393	25611	10971	1.94
	18.3	24515	24501	12180	2.01
	19.2	19982	20141	13448	1.70

mean	19.5	23324	23595	12056	1.94
St.dn.	1.0	2161	2005	834	0.13
COV	0.05	0.09	0.08	0.07	0.06
133_5 days curing					
M_6	24.8	25050	25217	12732	2.0
	23.5	21443	21868	15261	1.4
	27.4	29262	30052	13346	2.3
	27.7	25838	26657	14225	1.9
	28.1	27706	28034	13625	2.1
	27.5	26745	27398	14109	1.9
mean	26.5	26007	26538	13883	1.92
St.dn.	1.9	2676	2789	866	0.27
COV	0.07	0.10	0.11	0.06	0.14
133_2.5%AE-no curing					
M_7	12.1	21210	21243	8188	2.6
	9.9	18429	18571	7841	2.4
	11.9	22449	22999	7494	3.1
	12.1	18794	19273	7739	2.5
	11.7	18335	19075	7412	2.6
	10.8	19342	20353	5898	3.5
mean	11.4	19760	20252	7429	2.8
St.dn..	0.9	1688	1656	799	0.4
COV	0.08	0.09	0.08	0.11	0.15
133_3.5%AE-no curing					
M_8	12.3	21060	21556	10030	2.1
	10.5	21315	22784	9318	2.4
	12.1	13492	12547	8025	1.6
	10.2	18553	20406	7255	2.8
	10.8	16070	16812	8601	2.0
	11.2	20673	20434	7433	2.7
mean	11.2	18527	19090	8444	2.28
St.dn.	0.9	3168	3775	1087	0.48
COV	0.08	0.17	0.20	0.13	0.21
124_0.75 5 days curing (B)					
M_9	17.3	22027	22125	9463	2.3
	20.1	19923	20901	9235	2.3
	17.2	21614	22570	11282	2.0
	17.9	20097	19826	8735	2.3
	17.2	20841	21205	7020	3.0
	17.2	14780	13594	6848	2.0
mean	17.8	19880	20037	8764	2.31
St.dn.	1.1	2631	3300	1659	0.38
COV	0.06	0.13	0.16	0.19	0.16
124_0.75-14 days curing					
M_{10}	24.7	22182	22561	14314	1.6
	22.8	16136	16430	13990	1.2
	23.4	23467	23488	14897	1.6
	22.4	24027	24102	12191	2.0
	26.7	24252	21684	13956	1.6
	23.2	20822	21068	14206	1.5
mean	23.9	21814	21556	13926	1.56
St.dn.	1.6	3064	2748	915	0.26

COV	0.07	0.14	0.13	0.07	0.16
133_3.5 % AE-no curing Recy. Agg.					
M_{11}	12.0	16640	17622	7997	2.2
	13.0	13453	14281	9889	1.4
	15.7	17230	17685	10993	1.6
	16.6	21042	20282	8231	2.5
	13.4	12068	12393	10327	1.2
mean	14.1	16086	16453	9487	1.78
St.dn.	1.9	3509	3112	1316	0.53
COV	0.14	0.22	0.19	0.14	0.30
133_2.5% AE-no curing-Recy. Agg.					
M_{12}	16.5	20115	20631	10287	2.0
	14.2	17930	18565	8846	2.1
mean	15.3	19022	19598	9566	2.05
St.dn.	1.6	1546	1461	1019	0.07
COV	0.10	0.08	0.07	0.11	0.03
133_3.5% AE no curing normal Agg.					
M_{13}	18.5	20426	20591	12419	1.7
	14.9	21679	22170	12425	1.8
	16.8	19889	19814	11926	1.7
	13.5	17889	18177	9827	1.8
mean	15.91	19971	20188	11649	1.72
St.dn.	2.2	1577	1661	1237	0.07
COV	0.14	0.08	0.08	0.11	0.04

Table A.2. Statistical analysis of the concrete strengths and strains data at different locations in σ-ε curve for specimens in each mix

Mix	f_{cmax} (MPa)	f_{c85} (MPa)	ε_{cmax}	ε_{c85}	$f_{c,ult}$ (MPa)	$\varepsilon_{c,ult}$	α	strain error %
124_0.82-no curing								
M1	5.5	4.7	0.00142	0.01199	4.9	0.01166	0.89	-2.7
	7.4	6.3	0.00104	0.00312	6.4	0.00360	0.87	15.3
	8.6	7.4	0.00129	0.00299	7.2	0.00350	0.84	17.2
	10.4	9.0	0.00120	0.00291	8.6	0.00380	0.83	30.6
	7.0	6.0	0.00123	0.00318	6.0	0.00297	0.87	-6.5
mean	7.8	6.7	0.00126	0.00484	6.5	0.003440	0.84	2.3
St.dn.	1.8	1.6	0.00017	0.00434	1.2	0.001809	0.05	28.3
COV	0.2	0.2	0.13280	1.01763	0.2	0.525914	0.06	12.5
134_0.92-no curing								
M2	6.30	5.5	0.00107	0.00455	5.3	0.00457	0.85	0.5
	6.8	5.8	0.00139	0.00405	6.0	0.00380	0.87	-6.2
	6.2	6.2	0.00141	0.00141	4.9	0.00249	0.79	76.8
	5.4	4.6	0.00134	0.00314	4.8	0.00380	0.90	21.0
	6.5	5.6	0.00086	0.00340	5.9	0.0022	0.90	-35.3
mean	6.2	5.5	0.00122	0.00331	5.4	0.0034	0.86	11.4
St.dn.	0.5	0.6	0.00024	0.00120	0.5	0.0010	0.05	41.8
COV	0.1	0.1	0.19785	0.36131	0.1	0.2945	0.05	3.7
124_0.75-5 days curing (A)								
M3	15.0	12.8	0.00132	0.00301	12.1	0.00366	0.80	21.7
	13.8	11.7	0.00106	0.00226	11.0	0.00270	0.80	19.1

	14.8	12.6	0.00124	0.00406	12.4	0.00445	0.83	9.8
	15.9	13.6	0.00166	0.00375	13.2	0.00418	0.83	11.7
	12.4	10.6	0.00150	0.00391	11.0	0.00347	0.89	-11.2
	15.2	13.1	0.00161	0.00395	13.1	0.00372	0.86	-5.8
	15.1	12.9	0.00115	0.00272	12.3	0.00307	0.81	12.7
	13.3	11.4	0.00113	0.00292	11.1	0.00310	0.83	6.2
mean	14.5	12.3	0.00133	0.00332	12.0	0.0035	0.83	8.0
St.dn.	1.18	0.99	0.00023	0.00068	0.91	0.0006	0.03	11.42
COV	0.1	0.1	0.17266	0.20370	0.08	0.1663	0.04	1.4
134_0.75-5 days curing								
M4	14.1	12.0	0.00162	0.00457	11.8	0.00508	0.84	11.0
	13.6	11.7	0.00166	0.00343	11.5	0.00346	0.85	0.9
	12.9	10.9	0.00167	0.00409	10.8	0.00431	0.84	5.4
	11.6	10.0	0.00132	0.00351	9.4	0.00470	0.81	33.8
	15.0	12.8	0.00091	0.00351	12.6	0.00377	0.84	7.4
	14.1	12.1	0.00141	0.00332	12.5	0.00309	0.89	-6.9
mean	13.6	11.6	0.00143	0.00374	11.4	0.0041	0.84	8.6
St.dn..	1.2	1.0	0.00029	0.00049	1.19	0.0008	0.02	13.8
COV	0.09	0.08	0.20481	0.13089	0.10	0.1864	0.03	1.6
133_no curing								
M5	20.9	17.8	0.00171	0.00262	16.2	0.00295	0.78	12.9
	19.9	17.1	0.00173	0.00253	15.4	0.00279	0.78	10.1
	18.6	15.9	0.00155	0.00309	15.2	0.00351	0.81	13.8
	20.4	17.5	0.00186	0.00299	16.0	0.00341	0.78	14.0
	18.3	15.5	0.00150	0.00276	14.6	0.00308	0.80	11.6
	19.2	16.4	0.00142	0.00314	15.3	0.00393	0.80	25.3
mean	19.5	16.7	0.00163	0.00285	15.4	0.0033	0.79	14.6
St.dn.	1.0	0.9	0.00016	0.00025	0.56	0.0004	0.02	5.4
COV	0.1	0.1	0.10070	0.08878	0.04	0.1279	0.02	0.4
133_5 days curing								
M6	24.8	21.2	0.00194	0.00341	19.9	0.00391	0.80	14.6
	23.5	20.2	0.00154	0.00177	15.5	0.00228	0.66	28.9
	27.4	25.6	0.00205	0.00195	15.7	0.00276	0.57	41.6
	27.7	23.8	0.00195	0.00282	22.3	0.00310	0.80	9.8
	28.1	24.2	0.00206	0.00254	19.9	0.00269	0.71	6.1
	27.5	23.7	0.00195	0.00233	19.7	0.00269	0.72	15.6
mean	26.5	23.1	0.00192	0.00247	18.8	0.0029	0.71	19.4
St.dn.	1.9	2.0	0.00019	0.00060	2.7	0.0006	0.09	13.3
COV	0.1	0.1	0.10015	0.24273	0.1	0.1914	0.12	0.7
133_2.5% A.E-no curing								
M7	12.1	10.3	0.00147	0.00282	10.4	0.00381	0.86	35.0
	9.9	8.4	0.00126	0.00401	8.8	0.00356	0.89	-11.1
	11.9	10.3	0.00159	0.00284	9.7	0.00342	0.82	20.3
	12.1	10.4	0.00156	0.00295	9.7	0.00403	0.81	36.6
	11.7	10.0	0.00158	0.00305	9.8	0.00322	0.84	5.4
	10.8	9.5	0.00184	0.00298	8.8	0.00328	0.81	10.1
mean	11.4	9.8	0.00155	0.00311	9.5	0.0036	0.84	16.0
St.dn.	0.9	0.8	0.00019	0.00045	0.63	0.0003	0.03	18.4
COV	0.08	0.08	0.12102	0.14440	0.07	0.09	0.04	1.1
133_3.5% AE-no curing								
M8	12.3	10.5	0.00123	0.00312	10.5	0.0043	0.86	37.7
	10.5	9.2	0.00113	0.00285	8.9	0.0039	0.85	36.9

	12.1	10.4	0.00151	0.00283	9.0	0.0035	0.74	23.5
	10.2	8.7	0.00141	0.00349	8.9	0.0039	0.87	11.6
	10.8	9.2	0.00125	0.00324	9.2	0.0042	0.85	29.7
	11.2	9.5	0.00151	0.00326	9.4	0.00340	0.84	4.4
mean	11.2	9.6	0.00134	0.00313	9.3	0.0039	0.83	23.97
St.dn.	0.9	0.7	0.00016	0.00026	0.64	0.0004	0.05	13.6
COV	0.1	0.1	0.12021	0.08163	0.07	0.0935	0.05	0.6
124_0.75-5 days curing (B)								
M9	17.3	14.8	0.00183	0.00447	14.8	0.00380	0.85	-14.9
	17.9	15.2	0.00194	0.00456	15.1	0.00390	0.85	-14.4
	20.1	17.2	0.00178	0.00313	16.3	0.00339	0.81	8.6
	17.3	14.8	0.00198	0.00392	14.8	0.00389	0.86	-0.7
	17.2	14.6	0.00244	0.00606	14.3	0.00627	0.83	3.5
	17.2	14.6	0.00251	0.00628	14.8	0.00589	0.86	-6.2
mean	17.8	15.2	0.00208	0.00473	15.0	0.0045	0.84	-4.0
St.dn.	1.1	1.0	0.00031	0.00122	0.67	0.0012	0.02	9.6
COV	0.1	0.1	0.15139	0.25865	0.04	0.2710	0.02	-2.4
124_0.75-14 days curing								
M10	24.7	21.3	0.00173	0.00254	18.1	0.00304	0.73	19.4
	22.8	19.5	0.00163	0.00198	16.1	0.00310	0.71	56.7
	23.4	20.2	0.00157	0.00214	17.0	0.00253	0.73	18.1
	22.4	19.3	0.00184	0.00235	15.3	0.00253	0.68	7.7
	26.7	22.7	0.00191	0.00252	18.8	0.00304	0.71	20.6
	23.2	20.5	0.00164	0.00223	16.6	0.00231	0.71	3.9
mean	23.9	20.6	0.00172	0.00229	17.0	0.0028	0.71	21.1
St.dn.	1.59	1.27	0.00013	0.00022	1.28	0.0003	0.02	18.74
COV	0.07	0.06	0.07797	0.09660	0.08	0.1230	0.02	0.89
133-3.5 % AE-no curing Recy. Agg.								
M11	12.0	10.3	0.00150	0.00310	9.8	0.00339	0.81	9.3
	12.9	11.1	0.00131	0.00316	10.9	0.00326	0.84	3.2
	15.7	13.7	0.00142	0.00309	12.6	0.00317	0.81	2.8
	16.6	15.2	0.00202	0.00250	12.0	0.00279	0.72	11.3
	13.5	11.7	0.00130	0.00311	11.0	0.00378	0.81	21.5
mean	10.1	8.9	0.00108	0.00214	8.0	0.0023	0.6	6.9
St.dn.	1.9	2.0	0.00030	0.00027	1.1	0.0004	0.0	7.6
COV	0.2	0.2	0.27476	0.12830	0.1	0.1539	0.1	1.1
133-2.5% AE-no curing-Recy.Agg.								
M12	16.5	14.0	0.00160	0.00290	10.6	0.0036	0.65	24.1
	14.2	12.2	0.00160	0.00270	10.6	0.0037	0.75	37.0
mean	15.3	13.1	0.00160	0.00280	10.61	0.0037	0.70	30.6
St.dn.	1.6	1.3	0.00000	0.00014	0.03	0.0001	0.07	9.1
COV	0.1	0.1	0.00000	0.05051	0.00	0.0194	0.10	0.3
133_3.5% AE-5day curing normal Agg.								
M13	18.5	15.7	0.00149	0.00261	14.4	0.00278	0.78	6.3
	16.8	14.3	0.00140	0.00200	12.5	0.00320	0.75	60.0
	13.4	11.4	0.00136	0.00336	10.9	0.00386	0.81	14.9
mean	16.2	20.7	0.00212	0.00399	18.90	0.0049	1.17	40.59
St.dn.	2.60	2.21	0.00006	0.00068	1.79	0.0005	0.03	28.85
COV	0.16	0.11	0.03056	0.17080	0.09	0.1110	0.03	0.71

References

[1] A.J. Duranni, A.S. Elnashai, Y.M.A. Hashash, S.J. Kim, A. Masud, The Kashmir Earthquake of October 8, 2005, A Quick Look Report" Mid- America Earthquake Center, in, University of Illinois at Urbana-Champaign, 2005.
[2] A. Naseer, S.M. Ali, Z. Hussain, Reconnaissance Report on the 8th October, 2005 Earthquake Pakistan, in, Earthquake Engineering Centre, Department of Civil Engineering NWFP UET Peshawar, Pakistan, 2006.
[3] T. Nisikawa, Y. Nakano, Y. Tsuchiya, Y. Sanada, H. Sameshima, Quick report of damage investigation on buildings and houses due to October 8, 2005 Pakistan earthquake, in, Japan Society of Civil Engineers (JSCE) and Architectural Institute of Japan (AIJ) 2005.
[4] N. Peiris, T. Rossetto, P. Burton, S. Mahmood, EEFIT Mission: October 8, 2005 Kashmir Earthquake, in, 2005.
[5] Z.B. Koru, Seismic Vulnerability Assessment of Low Rise Reinforced Concrete Buildings, in, Purdue University, 2002.
[6] I.E. Bal, H. Crowley, R.F. Pinho, F.G. Gulay, Detailed assessment of structural characteristics of Turkish RC building stock for loss assessment models, Soil Dynamics and Earthquake Engineering, 28 (2008) 914–932.
[7] N. Kyriakides, Seismic Vulnerability Assessment of RC Buildings and Risk Assessment For Cyprus, in: Department of civil and structural engineering, The University of Sheffield, 2008.
[8] D.J. Carreira, K.D. Chu, Stress-Strain Relationship for Plain Concrete in Compression, ACI Journal, Proc 82(6) (1985) 797-804.
[9] CEB-FIP(MC90), CEB-FIP Model Code 1990: Design code, in, Comite Euro-International Du Beton(Ceb), 1993.
[10] EC2, Design of concrete structures-Part 1 General rules and rules for buildings (BS EN-1992-1-1:200), in, 2004.
[11] E. Hognestad, A study of combined bending and axial load in reinforced concrete members, in: Bulletin no 399, Engineering Experimental Station, , University of Illinois, USA., 1951.
[12] P. Kumar, A compact analytical material model for unconfined concrete under uni-axial compression, Materials' and Structures / Matrriaux et Constructions, 37 (2004) 585-590.
[13] J.B. Mander, M.J.N. Priestley, R. Park, Theoretical Stress-Strain Model for Confined Concrete, Journal of Structural Engineering (ASCE), 114 No.8 (1988) 1804-1826.
[14] S. Popovics, Numerical approach to the complete stress-strain curve of concrete Cement and Concrete research, 3 (1973) 583-599.
[15] J.F. Sima, P. Roca, C. Molins, Cyclic constitutive model for concrete, Engineering Structures, 30, Issue 3 (2008) 695-706
[16] W.T. Tsai, Uniaxial Compressional stress-strain relation of concrete, Journal of Structural Engineering (ASCE), 114 No 9 (1988) 2133-2136.
[17] R. Park, T. Paulay, Reinforced Concrete Structures: Chapter 6 - Ultimate Deformation and Ductility of Members with Flexure, John Wiley & Sons, 1975.
[18] I. Ashraf, Development of low strength concrete model and its implementation in in-elastic analysis, in: Department of Civil Engineering, UET, Taxila, Pakistan, 2008.
[19] S. Mindess, J.F. Young, D. Darwin, Concrete, Second edition ed., Prentice Hall, 2003.
[20] BS1881-121, Testing concrete -Part 121: Method for determination of static modulus of elasticity in compression, in, 1983.
[21] S. Ahmad, Seismic Vulnerability of Non-ductile Reinforced Concrete Structures in Developing Countries, in: Department of civil and structural engineering, The University of Sheffield, U.K., 2011.
[22] T. Ozturan, An investigation of concrete abrasion as two phase material(in Turkish). in: Faculty of Civil Engineering, Istanbul Technical University, 1984.
[23] M. Turan, M. Iren, Strain stress relationship of concrete, J Eng Arch (in Turkish), 12(1) (1997) 76–81.
[24] A.N. Ali, B.J. Farid, A.l.M. AL-Janabi, Stress-Strain Relationship for Concrete in Compression Made of Local Materials, JKAU: Eng Sci, 2 (1990) 183-194.

[25] S.T. Yi, J.K. Kim, T.K. Oh, Effect of strength and age on the stress–strain curves of concrete specimens, Cement and Concrete Research (2003) 1235–1244.
[26] ACI318, Building code requirements for structural concrete and commentary, in, 2005.
[27] TS500, Requirements for design and construction of reinforced concrete structures Turkish Standardization Institute, in, Ankara,Turkey, 2000.
[28] IS456, Plain and Reinforced Concrete - Code of Practice, Bureau of Indian Standards, in, New Delhi, 2000.
[29] M. Ros, Material-technological foundation and problems of reinforced concrete, Bericht No 162 (Eidgenossische Materialprfifungs und Versuchsanstalt f/Jr Industrie,Bauwesen and Gewerbe, Zurich, Switzerland, 1950), (1950).
[30] S. Popovics, Review of Stress-Strain Relationship for Concrete, ACI Journal, Proc, 67(3) (1970) 243-248
[31] L.P. Saenz, Discussion of Equation for the Stress strain curves for Concrete by Desai and Krishnan, ACI Journal, 61(9) (1964) 1229-1235.
[32] T.H. Wee, M.S. Chin, M.A. Mansur, Stress strain relationship of high strength concrete in compression, Journal of Materials in Civil Engineering (ASCE) 8(2) (1996) 70-76.
[33] K.K.B. Dahl, A Failure Criterion for Normal and High Strength Concrete, in: Project 5Rep56, , American Concrete Institute, Detroit., 1992.
[34] J. Ji, Seismic Fragility Assessment For Reinforced Concrete High rise buildings, in, UIUC, 2007.
[35] R. Kaul, Object oriented development of strength and stiffness degrading models for reinforced concrete structures, in, Stanford University, 2004.
[36] T. Rossetto, A.S. Elnashai, A new analytical procedure for the derivation of displacement-based vulnerability curves for population of RC structures, Engineering Structures, 27(3) (2005) 397-409.